Received: 28 July 2023 | Revised: 3 November 2023 | Accepted: 15 December 2023

DOI: 10.1002/prot.26657

RESEARCH ARTICLE

PROTEINS WILEY

Synergy and anti-cooperativity in allostery: Molecular dynamics study of WT and oncogenic KRAS-RGL1

Aysima Hacisuleyman[1] | Burak Erman[2]

[1]Department of Computational Biology, University of Lausanne, Lausanne, Switzerland

[2]Department of Chemical and Biological Engineering Koc University, Istanbul, Turkey

Correspondence
Burak Erman, Department of Chemical and Biological Engineering, Koc university, Istanbul, Turkey.
Email: berman@ku.edu.tr

Abstract

This study focuses on investigating the effects of an oncogenic mutation (G12V) on the stability and interactions within the KRAS-RGL1 protein complex. The KRAS-RGL1 complex is of particular interest due to its relevance to KRAS-associated cancers and the potential for developing targeted drugs against the KRAS system. The stability of the complex and the allosteric effects of specific residues are examined to understand their roles as modulators of complex stability and function. Using molecular dynamics simulations, we calculate the mutual information, MI, between two neighboring residues at the interface of the KRAS-RGL1 complex, and employ the concept of interaction information, II, to measure the contribution of a third residue to the interaction between interface residue pairs. Negative II indicates synergy, where the presence of the third residue strengthens the interaction, while positive II suggests anti-cooperativity. Our findings reveal that MI serves as a dominant factor in determining the results, with the G12V mutation increasing the MI between interface residues, indicating enhanced correlations due to the formation of a more compact structure in the complex. Interestingly, although II plays a role in understanding three-body interactions and the impact of distant residues, it is not significant enough to outweigh the influence of MI in determining the overall stability of the complex. Nevertheless, II may nonetheless be a relevant factor to consider in future drug design efforts. This study provides valuable insights into the mechanisms of complex stability and function, highlighting the significance of three-body interactions and the impact of distant residues on the binding stability of the complex. Additionally, our findings demonstrate that constraining the fluctuations of a third residue consistently increases the stability of the G12V variant, making it challenging to weaken complex formation of the mutated species through allosteric manipulation. The novel perspective offered by this approach on protein dynamics, function, and allostery has potential implications for understanding and targeting other protein complexes involved in vital cellular processes. The results contribute to our understanding of the effects of oncogenic mutations on protein–protein interactions and provide a foundation for

future therapeutic interventions in the context of KRAS-associated cancers and beyond.

KEYWORDS
Allostery, anti-cooperativity, dynamic allostery, interaction information, molecular dynamics, mutual information, oncogenic mutation, synergy, three-body interactions

1 | INTRODUCTION

The formation of protein complexes is governed by several factors, including their stability and the transmission of information between residues within the complex interface. These two aspects present critical considerations, as they greatly influence the functionality and regulatory potential of the complex. In this context, the KRAS-RGL1 protein complex presents itself as a compelling subject of investigation, as it encompasses both the challenges and opportunities associated with complex formation, stability, and allosteric information transfer. The stability of a protein complex is a crucial factor in determining its functional integrity, and when two proteins form a stable complex, there tends to be a high mutual information (MI) between the interface residues, which measures the correlation between their fluctuations. The interacting surfaces often have complementary shapes and specific amino acid residues that interact with each other which contribute to the stability of the protein–protein complex. However, an overly stable complex may have undesirable consequences for the system. Excessive stability can hinder the dynamic nature of the complex, impeding its ability to undergo conformational changes essential for regulatory processes, and most importantly it may extend its life span in an unwanted way. Conversely, insufficient stability may result in a fragile complex prone to dissociation or misfolding. Achieving an optimal balance of stability is essential to maintain the complex's functional flexibility, allowing it to respond efficiently to various cellular cues and environmental changes. In addition of MI, the transmission of allosteric information within a protein complex plays a vital role in modulating its activity and regulation. In the case of the KRAS-RGL1 complex, the transmission of allosteric information may modulate the lifetime of the complex enabling it to respond to cellular signals, triggering downstream signaling cascades that regulate key cellular processes.[1] Understanding the mechanisms underlying the transmission of allosteric information is crucial for unraveling the complex's functionality and identifying potential therapeutic targets.

In this study, we investigate the effects of an oncogenic mutation on the stability and interactions within the KRAS-RGL1 complex. Our analysis aims to identify the effect of mutation on the stability of the complex and the allosteric effects of specific residues and their potential as modulators of complex stability and function. We specifically investigate the interactions between two neighboring residues located at the interface of the complex and how a third residue in KRAS affects the allosteric synergy between them. This understanding is crucial for developing targeted drugs against the KRAS system, particularly in the context of KRAS-associated cancers.[2,3] Based on extensive molecular dynamics simulations, we calculate the MI of these neighboring residues to assess the strength and dependence of their interactions, taking into account the effects of modulating other KRAS residues and the oncogenic mutation. By doing so, we aim to gain insights into the underlying mechanisms of complex stability and function and potentially identify new therapeutic targets.

Studies on finding the effect of a third residue on the interaction between two neighboring residues is not new, having its origins in the alanine scanning mutagenesis work of Cunningham and Wells.[4] But the first information theoretic treatment of the problem was given by LeVine and Weinstein[5] (Below, we give several references to work that followed Reference[5]). Our work elaborates further in this direction. Mutual information is a measure of the amount of information that two residues share. In the context of protein–protein interactions, MI between the residues involved in the interaction[6,7] can be used to quantify the degree to which the fluctuations of one residue are correlated with those of the other residue. In this context, MI may be interpreted as a measure of the strength of the interaction between the two residues. Mutual Information can provide insights into the nature of the interaction between the interface residues, which in turn gives information on the stability of the complex. For example, if the MI between two interface residues is high, it suggests that their fluctuations are highly correlated and that their interaction is strong. This, in turn, could contribute to the thermodynamic stability of the complex by lowering the free energy of the system upon complex formation, that is, thermodynamic stability. Similarly, a strong interaction between the two residues could contribute to the mechanical stability of the complex by generating a network of interactions that can resist external forces, that is, mechanical stability. On the other hand, if the MI between the two residues is low, it suggests that their fluctuations are uncorrelated and that their interaction is weak. This could lead to a less stable complex, as the weak interaction may not provide sufficient thermodynamic or mechanical stability. However, it is important to note that the MI between two residues can be influenced by the presence of a third residue, which may either enhance or diminish the interaction. This influence can be quantified using the concept of interaction information, II. Interaction information is defined as the difference between the MI values in the absence and presence of the third residue. A positive value indicates anti-cooperativity, meaning the presence of the third residue weakens the interaction between the residue pair. Conversely, a negative value indicates synergy, indicating that the third residue enhances the interaction between the residue pair.

The problem of allostery in protein–protein interactions is essentially a three-body problem. The first paper on three-body interactions accurately presented in information theory language is by LeVine and Weinstein[5] where they introduced the NbIT analysis for quantifying n-body interactions. Several papers followed using the information theory-based analysis of allosteric mechanisms in different proteins by LeVine, Weinstein and collaborators,[8–18] and by other authors.[19–28] Notably, Karami et al.,[26] used an information theoretic approach called 'infostery' where they derived the effects of all possible mutations on binding for the system PSD95's third PDZ domain in complex with its ligand CRIPT. These are cases where three-body interactions between spatially distant residues dominate, as in the case of allostery in a complex where a third residue, far from the interface affects the binding stability of the complex. A common case is when the distant third residue undergoes a mutation and changes the strength and stability of the interface pair. Several known examples may be found from databases such as SKEMPI[29] which reports results of 3047 $\Delta\Delta G$ measurements of 2792 unique sets of mutations from 158 structures of 85 protein–protein complexes. Similarly, the ASE[30] and PINT[31] databases contain information on 26 and 32 systems, respectively.

In the present paper, using the tools of information theory, we study the allosteric interactions of one of the most widely studied proteins, KRAS, and one its complexes. As of 2023, there are over 70 000 papers published on the topic of KRAS, covering experimental, computational, and clinical aspects of the system.[32–41] The interaction of KRAS with other proteins and the allosteric effect of modulating distant residues, such as by mutation or drug action, are emerging as important areas of study in the field of KRAS research. Accordingly, we investigate allosteric effects, specifically anti-cooperativity and synergy, resulting from the modulation of KRAS residues on the binding characteristics of both wild-type and oncogenic KRAS-RGL1 complexes.[1] RGL1 is a member of the Ral GTPase family proteins which binds to KRAS and shuttles it from the cytosol to the plasma membrane. Among several oncogenic mutations of KRAS, the G12V mutation, observed in non-small cell lung cancer, for example, is known to lead to higher Ral GTPase activation compared to those with wild type KRAS. Recently, it was shown[42] that G12C mutations of KRAS stabilizes the active conformation of KRAS, which enhances its ability to interact with downstream effectors and promote signaling.[43] In this first of a series of papers, we use molecular dynamics and an information theoretical approach to understand the effects of G12V mutation on the intrinsic binding features of RGL1 on KRAS. We see that there is a strong effect of G12V mutation on the stability of the complex, albeit in the undesirable direction.

The approach and the strategy of the paper is as follows: In the first part we evaluate mutual information values for the interface residues of the KRAS-RGL1 complex, for the wild type and the G12V mutated complexes for which accurate crystal structures are recently determined.[1] In the second part, we consider the allosteric regulatory effect of third residues on the stability of interface residue pair interactions in the two complexes, WT and G12V mutated. In the third part, we investigate the allosteric regulatory effect of third residues whose fluctuations are perturbed. All calculations are based on multivariate Gaussian distributions obtained from molecular dynamics trajectories of the complex. Among thousands of known mutations of KRAS, we focus on the G12V mutation only because the G12V mutation in the KRAS gene holds significant scientific and clinical relevance due to several compelling reasons.[33] Firstly, the G12V mutation is one of the most prevalent KRAS mutations found in various cancers, including colorectal, lung, and pancreatic cancer, which collectively account for a substantial proportion of cancer-related deaths worldwide. Its prevalence underscores its clinical importance and the urgent need to understand its molecular mechanisms. Second, G12V, characterized by the substitution of glycine with valine at codon 12, results in a unique alteration in the KRAS protein structure, which has been associated with a distinct signaling property that drives oncogenic processes, namely the mutation makes the complex over stable contrary to the general trend that allosteric mutations inhibit binding to effectors.[44] Thirdly, G12V is notorious for conferring resistance to certain targeted therapies, posing a significant challenge in cancer treatment. Therefore, elucidating the functional consequences and signaling pathways associated with the G12V mutation is vital for developing more effective treatment strategies and improving patient outcomes. Finally, accurate crystal structures of 1.96 Å rmsd KRAS-RGL1 complex have been published very recently which is highly significant from a computational perspective as it provides experimental validation for computational models, enhances structural insights, aids in drug design for targeted therapies, and enables more precise molecular dynamics simulations to understand the mutation's impact on protein behavior and cancer development.

2 | METHODS

2.1 | Molecular dynamics simulations

The structures of wild type (WT) KRAS-RGL1 complex (PDB ID: 7SCW) and G12V mutant KRAS-RGL1 complex (PDB ID: 7SCX) were used for the MD simulations with their bound GSP molecules. The systems were prepared by using CHARMM-GUI.[45] Each system was solvated in a TIP3P water box[46] with 15 Å of water between the protein surface and the periodic box edge. Na and Cl atoms were added to neutralize the system with a NaCl concentration of 150 mM. CHARMM36 force field was used in all MD simulations with a time step of 2 fs. The simulations were performed with explicit solvent in the NpT ensemble, with a distance cut-off of 12.0 Å applied to short-range, non-bonded interactions. The temperature was maintained at 310 K using Langevin dynamics The pressure was maintained at 1 atm using Nosé-Hoover Langevin piston.[47] All simulations were performed with NAMD 3.alpha13.[48]

For each system three replicas of simulations were run. First, each replica was minimized for 10 000 steps and equilibrated for 125 000 steps. After the equilibrations, each replica was run for 100 ns. Frames in each trajectory were aligned to the first frame of the simulation by using VMD to eliminate all rotational and translational degrees of

freedom and the analysis is done with the aligned Cartesian coordinates of the Cα atoms. The trajectory was saved with a stride of 10 and the analysis is done on 5000 time points. All calculations reported below are from trajectories obtained by combining the three replicas. Results from individual replicas are observed to duplicate the combined trajectories with Pearson correlation coefficient larger than 0.95 (see Figure S28).

2.2 | Extracting information from molecular dynamics time series

The fluctuation vector for the residues of interest is defined by the column vector ΔR

$$\begin{aligned}\Delta R_{ij\ldots n}(t) &= col\left[\Delta R_i(t)\Delta R_j(t)\ldots.\ \Delta R_n(t)\right]\\ &= col[\Delta X_i(t)\ \ \Delta Y_i(t)\ \ \Delta Z_i(t)\ \ \Delta X_j(t)\ \ \Delta Y_j(t)\ \ \Delta Z_j(t)\ \ \ldots\\ &\Delta X_n(t)\Delta Y_n(t)\Delta Z_n(t)]\end{aligned} \tag{1}$$

Here, col indicates column, $\Delta X_i(t)$, $\Delta Y_i(t)$ and $\Delta Z_i(t)$ denote the Cartesian components of the fluctuation of residue i at time t. All coordinates are obtained from the 5000 time points of the molecular dynamics trajectory. For 1, 2, and 3 residues, for each time point, $\Delta R(t)$ is of dimensions 3×1, 6×1 and 9×1, respectively. All averages are over the 5000 time points. From here on, the time argument will be suppressed for brevity.

2.3 | Definitions of information theoretic functions

The Shannon entropy, H for n residues is:

$$H(\Delta R_1,\Delta R_2,\ldots,\Delta R_3) = -k_B\langle \log p(\Delta R_1,\Delta R_2,\ldots,\Delta R_3)\rangle \tag{2}$$

where p is the joint probability for the fluctuations ΔRi of n residues. The probability of a variable X from the trajectory is defined by recording all instantaneous values of X, forming a histogram and writing the function $p(X)$ that represents the histogram. The angular brackets in Equation (2) is an average over all values of the fluctuations. In Shannon's notation, the log is to base 2 and the constant k is unity. When k is the Boltzmann constant, k_B, and the log is the natural logarithm, H becomes identical with the thermodynamic entropy (see e.g., Callen[49]). In the following, we will take $k_B = 1$ and the natural logarithm. Accurate construction of the probability function of three arguments from molecular dynamics trajectories requires trajectories in the order of microseconds even for a small protein. Multivariate Gaussian approximation reduces this demand on trajectory length to the order of 100 nanoseconds[50] as we discuss in more detail below.

Mutual information is defined as:

$$I(\Delta R_i,\Delta R_j) = H(\Delta R_i) + H(\Delta R_j) - H(\Delta R_i,\Delta R_j) \tag{3}$$

Given the third residue k, it is:

$$I(\Delta R_i,\Delta R_j|\Delta R_k) = H(\Delta R_i|\Delta R_k) + H(\Delta R_j|\Delta R_k) - H(\Delta R_i,\Delta R_j|\Delta R_k) \tag{4}$$

where $I(\Delta R_i,\Delta R_j|\Delta R_k)$ is the conditional MI, CMI.

How much MI between residues i and j will change due to the effect of k is given by II defined as:

$$II(\Delta R_i;\Delta R_j;\Delta R_k) = I(\Delta R_i;\Delta R_j) - I(\Delta R_i;\Delta R_j|\Delta R_k) \tag{5}$$

Our calculations on the KRAS-RGL1 complex reported below show that II is predominantly positive, that is, anti-cooperative. In this case, II competes with MI. In terms of entropies, II reads as:

$$\begin{aligned}II(\Delta R_i,\Delta R_j,\Delta R_k) = {} & H(\Delta R_i,\Delta R_j,\Delta R_k) - H(\Delta R_i,\Delta R_j)\\ & - H(\Delta R_i,\Delta R_k) - H(\Delta R_j,\Delta R_k) + H(\Delta R_i)\\ & + H(\Delta R_j) + H(\Delta R_k)\end{aligned} \tag{6}$$

A positive value indicates the degree of anti-cooperativity induced by k to the interaction of i and j. Conversely, if the value is negative, it is the synergy. The derivation of Equation (6) is given in Data S1.

2.4 | Multivariate Gaussian Approximation to Interaction Information

The presence of $H(\Delta R_i,\Delta R_j,\Delta R_k)$ in Equation (6) necessitates the evaluation of third order probabilities from a molecular dynamics trajectory, which requires a large number of data points which in turn requires simulations in the order of microseconds for accurate representation. Recently, it was shown that[50] multivariate Gaussian representations to higher order probability functions serve as a suitable approximation to functions obtained from microsecond long trajectories. In Data S1, we elaborate on this point and obtain the Gaussian approximation to II as:

$$\begin{aligned}&II(\Delta R_i,\Delta R_j,\Delta R_k)\\ &= \frac{1}{2}\left\{\log\left[\frac{\det\langle\Delta R_i\Delta R_j{}^T\rangle\det\langle\Delta R_j\Delta R_j{}^T\rangle\det\langle\Delta R_k\Delta R_k{}^T\rangle\det\langle\Delta R_{ijk}\Delta R_{ijk}{}^T\rangle}{\det\langle\Delta R_{ij}\Delta R_{ij}{}^T\rangle\det\langle\Delta R_{ik}\Delta R_{ik}{}^T\rangle\det\langle\Delta R_{jk}\Delta R_{jk}{}^T\rangle}\right]\right\}\end{aligned} \tag{7}$$

Here, det represents the determinant of its argument, where $\langle\Delta R_i\Delta R_j{}^T\rangle$, $\langle\Delta R_{ij}\Delta R_{ij}{}^T\rangle$ and $\langle\Delta R_{ijk}\Delta R_{ijk}{}^T\rangle$ are matrices of order 3, 6, and 9, respectively. Evaluation of these averages using probability functions requires microsecond long trajectories whereas a comparable accuracy is obtained from 100 ns trajectories when Gaussians are used, notably due to the central limit theorem.

The multivariate Gaussian forms of MI and conditional MI are

$$I(\Delta R_i;\Delta R_j) = -\frac{1}{2}\log\left(\frac{\det\langle\Delta R\Delta R^T\rangle}{\det\langle\Delta R_i\rangle\det\langle\Delta R_j\rangle}\right) \tag{8}$$

$$I(\Delta R_i;\Delta R_j|\Delta R_k)=\frac{1}{2}\log\left[\frac{\det\langle\Delta R_{ik}\Delta R_{ik}{}^T\rangle\det\langle\Delta R_{jk}\Delta R_{jk}{}^T\rangle}{\det\langle\Delta R_{ijk}\Delta R_{ijk}{}^T\rangle\det\langle\Delta R_k\Delta R_k{}^T\rangle}\right] \quad (9)$$

The derivations of Equations (7–9) are given in Data S1.

2.5 | Covariance matrix based correlations and general relations between mutual information, dynamic coupling, dynamic flexibility, and stability

Mutual information is a useful metric for quantifying cooperativity and stability of binding in terms of correlations between fluctuations of residues.[51] That MI is directly related to correlation of residue fluctuations can be seen by expanding the determinant in Equation (8) and expanding the logarithmic term into Taylor's series as

$$I(\Delta R_i;\Delta R_j)=-\frac{1}{2}\log\left(1-\frac{\langle\Delta R_i\Delta R_j\rangle^2}{\langle(\Delta R_i)^2\rangle\langle(\Delta R_j)^2\rangle}\right)\approx\frac{\langle\Delta R_i\Delta R_j\rangle^2}{\langle(\Delta R_i)^2\rangle\langle(\Delta R_j)^2\rangle}+\ldots \quad (10)$$

This approximation enables the development of several metrics of cooperativity based on correlations. A recently used metric in the literature, for example, is the Dynamic Coupling Index,[52,53] DCI_{ij}, which measures the response of residue i upon perturbation of functional residues in the protein. This model derives from the Perturbation-response scanning model[54] which is an application of the more general linear response theory, LRT, which in turn is obtained from the Onsager relation of fluctuations[49]

$$\langle\Delta R_i\Delta R_j\rangle=k_BT\left(\frac{\partial R_i}{\partial F_j}\right) \quad (11)$$

where k_B is the Boltzmann constant, T is the absolute temperature, R_i is the instantaneous position of residue i and F_j is the force acting on residue j. When multiplied by force F_j and summed over j, Equation (11) takes the familiar form:[55]

$$dR^j{}_i=(k_BT)^{-1}\sum_j\langle\Delta R_i\Delta R_j\rangle dF_j \quad (12)$$

where $dR^j{}_i$ is the response fluctuation of residue i upon perturbation of residue j. We have written Equation (12) in one dimension to show the principle, extension to three dimensions as was done in Reference[54] is simply a matter of straightforward approximation. Thus, $dR^j{}_i$ becomes the basis of a metric that quantifies cooperativity or flexibility. Equation (12) may be normalized in order to get rid of the force, as a result of which we obtain the Dynamic Coupling Index, DCI, of Ozkan and collaborators[41,53] as:

$$DCI_{ij}=C_0\left|\Delta R^j\right|_i=C_0\sum_i\left|\langle\Delta R_i\Delta R_j\rangle dF_j\right| \quad (13)$$

where, C_0 is a normalization constant, and the sum is over the functionally critical residues in the protein. A plausible but not the only choice of the normalization constant may be chosen for a unit force as $\left[\left\langle(\Delta R_i)^2\right\rangle\left\langle(\Delta R_j)^2\right\rangle\right]^{-0.5}$ which we adopted below in obtaining Figure 2. The choice of the normalization constant will change the amplitude of the DCI only. Ozkan et al. randomized the force by taking an average over several randomly chosen forces. This makes the problem consistent with the solution of the Langevin equation where the random perturbing forces come from white noise.[56]

Along similar lines, another metric, total coupling:

$$C_{ij}(k)=\left\langle\sum_m\Delta R_i(k)\Delta R(m)\right\rangle \quad (14)$$

was used as a metric of stability of binding protein complexes.[57] Here, the fluctuations are expressed in terms of their modal components and k and m represent the mode numbers. First dominant collective modes are known to relate to function whereas fast modes, which are associated with hinges by some authors, relate to stability of binding.[41,57,58] Equations (10, 12, 13, 14) are simple power transformations of the covariance matrix. Lange and Grussmuller[59] showed that the use of covariance matrix misses more than 50% of the correlations. In summary, all these metrics reflect a particular aspect of the correlation matrix. Full generality is only obtained with the use of the expression (see Data S1)

$$I(\Delta R_i;\Delta R_j)=\left\langle\log\left(\frac{p(\Delta R_i,\Delta R_j)}{p(\Delta R_i)\,p(\Delta R_j)}\right)\right\rangle \quad (15)$$

where $p(\Delta R_i,\Delta R_j)$ is the joint probability of the fluctuations of residues i and j. A straightforward way of determining the joint probability is to perform molecular dynamics simulations. However, determination of $p(\Delta R_i,\Delta R_j)$ which is a six-dimensional function in Cartesian components requires micro to millisecond trajectories depending on the size of the system. Therefore, recourse to simplified expressions based on the correlation matrix becomes inevitable. An alternative method of expressing mutual information in terms of Hermite series was proposed recently,[60] which requires the evaluation of higher moments of the covariance matrix.

In summary, covariance matrix based mutual information metrics seem to be the most feasible common metric for all practical purposes.

2.6 | Dynamic nature of interactions and uncertainty

Both mutual information and interaction information are dynamic quantities derived here from molecular dynamics simulations, which model the movements and interactions of atoms in the protein

complex over time. The process of molecular dynamics inherently involves small, random fluctuations in the positions of individual amino acid residues within the complex. These fluctuations arise due to the constant thermal motion of atoms and introduce a certain level of uncertainty to the problem. Mutual information measures how these fluctuations become less uncertain when two residues interact and influence each other's movements. On the other hand, interaction information measures the increase in uncertainty when the interaction between two residues is influenced by a third residue. This dynamic aspect of interaction information is particularly relevant in capturing the dynamic nature of allostery, where distant residues can affect the stability and behavior of the protein complex. Throughout the paper, we will use the term 'increase in uncertainty' to refer to interaction information, and it will be understood that these measures originate from molecular dynamics simulations that simulate the dynamic motions of the protein complex.

2.7 | Factors affecting the change of MI in protein complexes

Allosteric regulatory effect of third residues on the stability of interface residue pair interactions.

We now consider specifically two neighboring interface residues *i* in KRAS and *j* in RGL1 and consider the effect of any third residue *k* in KRAS and discuss the molecular factors that increase or decrease MI for the interaction of *i* and j:

1. Synergy: If the presence of *k* decreases the uncertainty in the interaction of *i* and *j*, we say that the allosteric effect of *k* on the interaction of *i* and *j* is synergistic. This can be explained by reference to allosteric regulation, for example, where residue *k* acts as an allosteric effector, influencing the interaction between *i* and *j* through indirect interactions with other residues in the protein. The dynamic coupling or conformational coupling of *k* to the interface occurs when the fluctuations of *k* correlate with the fluctuations of residues *i* and/or *j*, typically facilitated by hydrogen bonds, salt bridges, or other non-covalent interactions. Strongly coupled interactions and similar timescales of fluctuations enhance the correlation between *k* and *i* and/or *j*.
2. Anti-cooperativity: If the presence of *k* increases the uncertainty in the interaction of *i* and *j*. Several sources may induce anti-cooperativity some of which are:
   i. Covalently bonded neighbor effect: Molecular dynamics results presented below show that the uncertainty in the interaction of *i* and *j*, (*i* in KRAS and *j* in RGL1) when the third KRAS residue *k* is covalently bonded to *i* in KRAS increases. Normally, when two residues are not covalently bonded, they are free to move independently of each other. However, in the present example, *k* is covalently attached to *i* and cannot move far away from it. Now, imagine that the protein environment changes and causes residue *i* to undergo changes in its fluctuations. Because *k* is bonded to *i*, it will also be affected by these changes and will move along with *i*. However, in the absence of the covalent bond, *k* would not necessarily be near *i* and could wander away by random forces from the environment. Therefore, k's natural fluctuations would not necessarily follow those of *i*. In fact, the fluctuations of *k* may be such that it would try to move away from *i*, in order to seek a more energetically favorable state. This is what we mean by anti-cooperativity, where the fluctuations of residue *k* are counterproductive to those of its neighboring residue *i*, which is held in place by a covalent bond. This can have important implications for the interaction between *i* and *j*, leading to increase of uncertainty between *i* and *j* given *k*.
   ii. The presence of noise-like fluctuations of *k* can affect the mutual interaction between the two dependent random variables, *i* and *j*, in several ways. First, the noise *k* can introduce random fluctuations in the values of *i* and *j*, which can affect their correlation and mutual interaction. If the noise *k* is correlated with either *i* or *j*, it can create spurious correlations or mask true correlations between *i* and *j*, known as confounding. Moreover, residue *k* can affect the strength of the correlation between *i* and *j*, when the noise *k* is relatively large compared to the magnitude of the correlation between *i* and *j*, it can weaken or even eliminate the correlation altogether. This is because the noise *k* introduces additional randomness that can obscure the underlying correlation between *i* and *j*. In such cases, II will be positive.
   iii. Non-noise-like fluctuations of *k* may mask the interaction between *i* and *j*. Masking of the interaction between residues *i* and *j* due to the presence of the fluctuations of residue *k* means that the dynamic behavior or fluctuations of residue *k* have an effect that obscures or diminishes the direct interaction between residues *i* and *j*. In the interface, residues *i* and *j* interact with each other through van der Waals forces, hydrogen bonds and salt bridges all of whose strength depend on the fluctuations, that is, dynamic in nature. However, when residue *k* undergoes fluctuations or dynamic changes, it can introduce additional factors or perturbations that influence the interaction between *i* and *j*. The presence of fluctuating residue *j* can disrupt or modulate the interaction between *i* and *j* by altering their spatial arrangement, altering the energetics of the interaction, or introducing competing interactions. As a result, the direct interaction between *i* and *j* may become less prominent or less detectable.

3 | RESULTS

Eves et al.[1] have conducted a comprehensive analysis of the structural characteristics of the interface formed by neighboring pairs Q25-N695, E31-N722, D33-K700, D33-K720, P34-K720, E37-R688, E37-I699, E37-S701, D38-I699, D38-S701, S39-M698, S39-I699, R41-N695, and R41-G696. We focus on examining the MI levels of these pairs, and on the allosteric effects induced by third residues in KRAS.

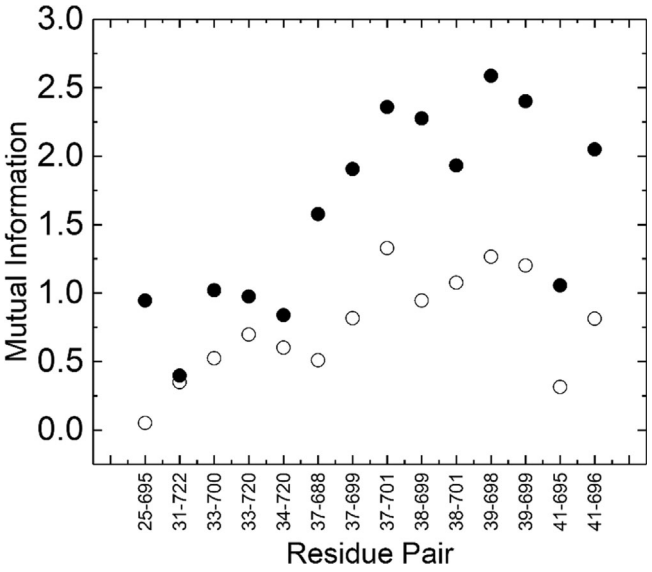

FIGURE 1 Values of MI for interface residue pairs for wild type KRAS (empty circles) and G12V variant (filled circles) calculated using Equation (8). The interface residues are identified along the abscissa.

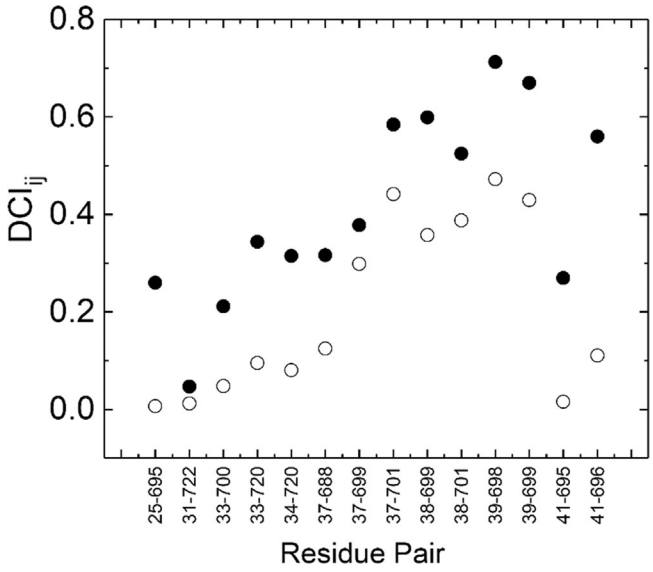

FIGURE 2 Values of Direct Coupling Index, DCI, for wild type KRAS (empty circles) and G12V variant (filled circles) calculated using Equation (13). The interface residues are identified along the abscissa.

3.1 | Part 1: Mutual Information

Mutual Information indicates that the G12V variant is more stable: Figure 1 compares the MI values of the interacting interface residue pairs for the wild type and G12V variant. In all cases MI values for the G12V variant are larger. Thus, the mutation makes a more stable complex which is known to lead to disease[1] by continuous constitutive activation of the protein, driving uncontrolled cell growth and proliferation.[61–63] According to the experimental findings of Eves et al[1] the G12V mutation stabilizes the overall structure of KRAS. This is evident from the observation that the root mean square deviation (RMSD) of the KRAS backbone atoms is lower in the G12V mutant complex than in the wild-type complex. The RMSD is a measure of the structural deviation of a protein from its reference structure. A lower RMSD indicates a more stable structure.

Based on linear response theory arguments, we proposed that the magnitude of correlations may be taken as an indication of stability. Accordingly, the right hand side of Equation (10) may be used as a simple measure of stability, which are plotted in Figure 2 Comparison of Figures 1 and 2 shows that the points obtained by the simple expression given by Equation (10) closely follow the pattern of the more accurate mutual information expression.

3.2 | Part 2: Allosteric regulatory effect of third residues on the stability of interface residue pair interactions

In Part 1, we examined the interactions of residue pairs at the interface to understand how they contribute to the stability of complex formation. In this section, we investigate how third residues in KRAS affect the interactions of interface residue pairs. We refer to this effect as allosteric action. We find that third residues generally decrease the stability of binding, but the dominant factor in the stability of the KRAS-RGL1 complex is due to the mutual information of the residue pairs, which we calculated in the previous section.

Here, we evaluate the changes in MI of interface residue pairs due to the allosteric effect of a third residue of KRAS. We do this for the wild type and the G12V variant and compare the two. Figure 3 compares the MI for Q25-N695 interface pair, represented by the horizontal line in each panel, with the conditional mutual information, CMI values obtained in the presence of the third residues. Third residues are indicated along the abscissa. The solid line shows the CMI values calculated using Equation (9). The horizontal line in the left panel indicates a small amount of MI. The CMI curve shows values both above and below the MI line, the ones above indicating synergy and the ones below indicating anti-cooperativity. For example, residue 21 has the highest synergetic effect on the interaction of Q25 and N695, whereas residue 41 has the highest anti-cooperative effect on the interface pair. The right panel for the G12V variant on the other hand shows a large value of MI indicating stronger interaction between Q25 and N695. The CMI curve in this panel falls below the MI line, showing that the third residues are decreasing the interaction between Q25 and N695, that is, allosterically anti-cooperative. MI value for the wild type is small, 0.052, while that for the G12V is 0.94. This shows that mutation increases the correlation between the two interface values significantly, but allosteric effects shown by MI conditioned on the third residues are all anti-cooperative in the G12V variant. The lower curve on the right panel shows that strongest anti-cooperative effects are by the two near neighbors 22 and 24 of 25 on KRAS. The next residue with the highest anti-cooperativity is residue 40 and then residue 57.

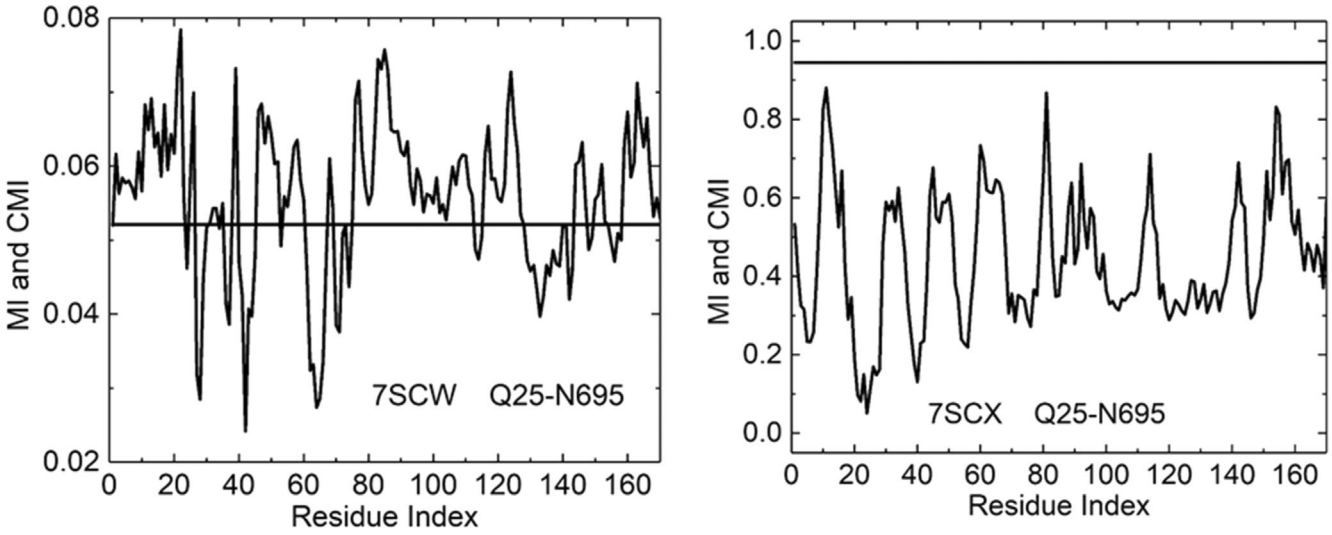

FIGURE 3 MI and CMI values for the interface pair Q25-N695 for the wild type (left panel) and the G12V mutant (right panel). Equations (8 and 9) are used, respectively, for calculating the values of MI and CMI for a third residue and this is repeated for all residues of KRAS.

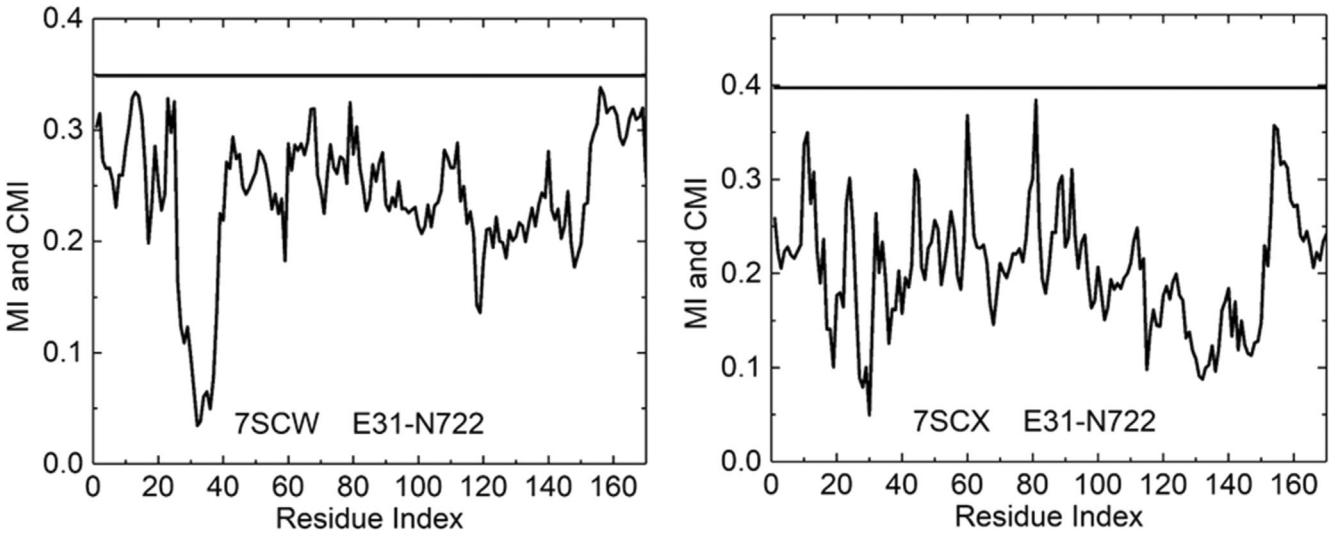

FIGURE 4 MI and CMI values for the interface pair E31-N722 for the wild type (left panel) and the G12V mutant (right panel). See legend to Figure 3.

Values of MI and CMI are compared for the interface pair E31-N722 as shown in Figure 4. It is interesting to note that for this pair, the magnitudes of MI values for the WT and G12V variant are comparable and the allosteric effect of third residues are all anti-cooperative.

The anti-cooperative effect of third residues can best be understood in terms of interaction information plots, which show the difference between MI and CMI. A large positive value of interaction information shows how much the third residues weaken the interaction between the interface residue pairs. Figure 5 displays this analysis for the interface pair Q25-N695. The curves are obtained for multivariate Gaussian approximation by using Equation (7). The lower black curve is for the wild type and the upper gray curve is for the G12V variant, obtained by using the PDB structures 7SCW and 7SCX, respectively. The abscissa values indicate the third residue for which calculations are conducted one by one for all residues except the interacting pair by using Equation (7). Results for the wild type indicate positive (anti-cooperative) and negative (synergistic) effects of the third residue, both of which are small. The gray curve for the G12V variant, on the other hand, is all positive and exhibits large anti-cooperativity. Thus, in this case, allosteric effect from third residues all decrease the interaction between Q25-N695. If one takes k_B as the Boltzmann constant, the energy equivalent of the ordinate values in Figure 4 will be in the order of about 0.5 k_BT. Figure 6 is obtained similarly for the interface pair E37-Y699. Changes in the interaction for all of the interface pairs under allosteric activity of third residues are superposed in Figure 7.

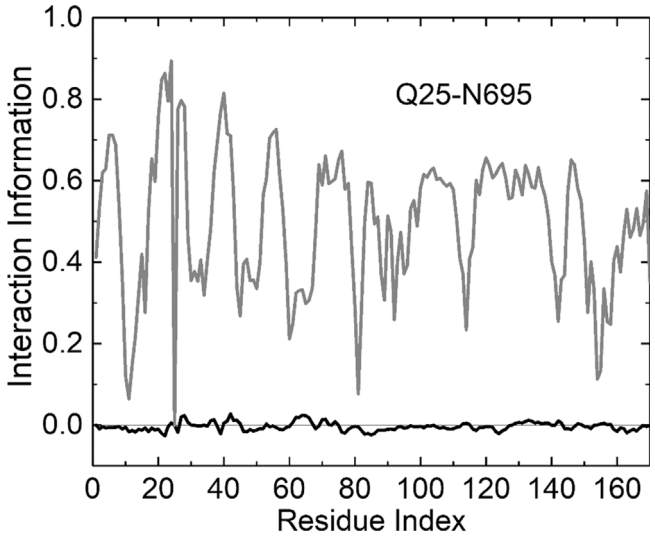

FIGURE 5 Interaction information values for Q25 and N695 under the allosteric effect of various residues shown along the abscissa. Black curve for wild type, gray curve for the G12V variant. All curves are calculated using Equation (7).

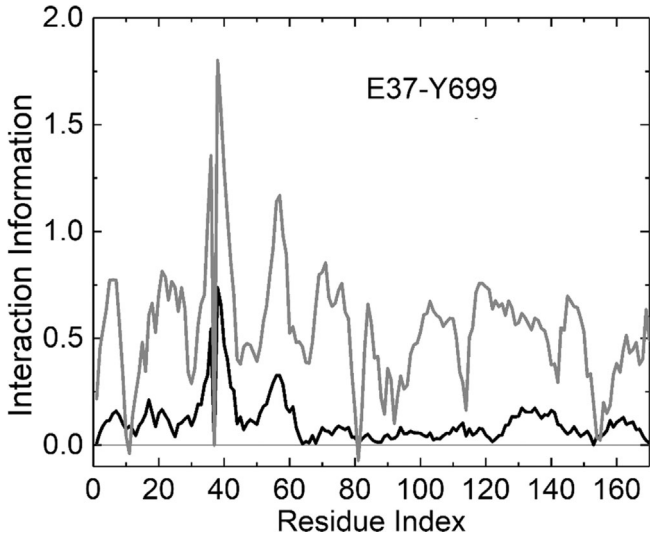

FIGURE 6 Interaction information values of E37 and Y699 under the allosteric effect of third residues shown along the abscissa. Black curve for wild type, gray curve for the G12V variant.

Figures 5–7 illustrate the contrasting effects of residue *k* on the activity of the wild type WT structure and the G12V variant. Figures similar to Figures 5 and 6 for the remaining interface residues pairs are presented in Figures S14–S27 in the Data S1 where values of CMI are plotted as a function of third residues. Across all figures, a consistent trend emerges wherein the presence of a third residue, say *k*, when covalently bonded to interface residue *i* of KRAS, acts as an anti-cooperative factor in the interaction between *i* and *j*. By examining these figures, it becomes evident that the effect of residue *k* tends to disrupt the interaction between residues *i* and *j*, resulting in reduced cooperation between them. This anti-cooperative effect suggests that the presence of residue *k* hampers the formation or stability of the i-j interaction, influencing the allosteric communication within the KRAS-RGL1 system. Thus, the anti-cooperative effects of third residues weaken the stabilizing effect of MI. This weakening effect is stronger for the G12V variant but the MI effect is even stronger in the variant, making the variant more stable than the wild type. Covalently bonded neighbor anti-cooperative effect is significant for all interface residue pairs. Synergy induced by allostery on the interface residues is negligibly small. Synergy effect in Figures 5 and 6, and in the remaining Figures S1–S13 presented in Data S1, are almost non-existent. The small extent of synergy can be seen from Figure 6; residue 11 in G12V has a weak synergistic effect on the E37-Y699 interface pair. Likewise, residue 81 exhibits also a weak synergistic effect on the same interface pair. In conclusion, we can say that in general the allosteric effect of third residues weaken the interaction between surface residue pairs of the KRAS-RGL1 complex.

Constraining the fluctuations of third residues increases the stability of the complex. In order to further understand the allosteric effect of constraining fluctuations of third residues on interface residue interactions, we perturbed the fluctuations of third residues and investigated the effect of this perturbation on the conditional MI between the interface residues. The perturbation is implemented in Equation (9) where the averages that involveΔR_k's are evaluated by using $0 \le \Delta R_k \le 0.3$ and all ΔR_k's larger than 0.3 equal to zero. This corresponds to conditioning the ΔR_k's which may mimic, for example, the action of a large ligand docked to residue *k*, decreasing its fluctuations. Constraining the fluctuations of the third residue stabilizes the interaction of the interface residues. Results of calculations are shown in Figures 8 and 9. The black line is for no constraint on third residues, the gray line for constrained third residues. Interestingly, Figure 8, left panel shows that the gray line falls below the black line at several points, indicating decrease in stability when third residues are constrained. However, the interaction of Q25 and N695 is weak where the MI equates to 0.053. For the G12V variant, the MI value for the 225-N695 pair is 0.92 and the gray line on the right panel of Figure 8 is close to the corresponding MI values. Thus, constraining third residues makes CMI approach MI and consequently the II decreases and the stability of the complex increases.

Mutation G12V leads to higher synergy for several residue pairs of KRAS. Here, we searched for the synergetic effect of G12V mutation on all residue pair interactions. In Figure 10 synergy values, that is, negative values of II from Equation (7) between three residues *i*, *j*, *k* for $k = 12$ are shown. This shows the allosteric effect of residue 12 on the residue pairs in the protein. The abscissae span the values of *i* and the ordinates span the values of *j*. The left panel is for the wild type and the right panel for the G12V variant. In the wild type, synergy values vary between 0 and −0.03 whereas for the G12V variant they vary between 0 and −0.09. The plots are drawn at intervals of 0.008. Although a value of −0.09 is small, nevertheless we see a totally different behavior in the two systems shown in Figure 10.

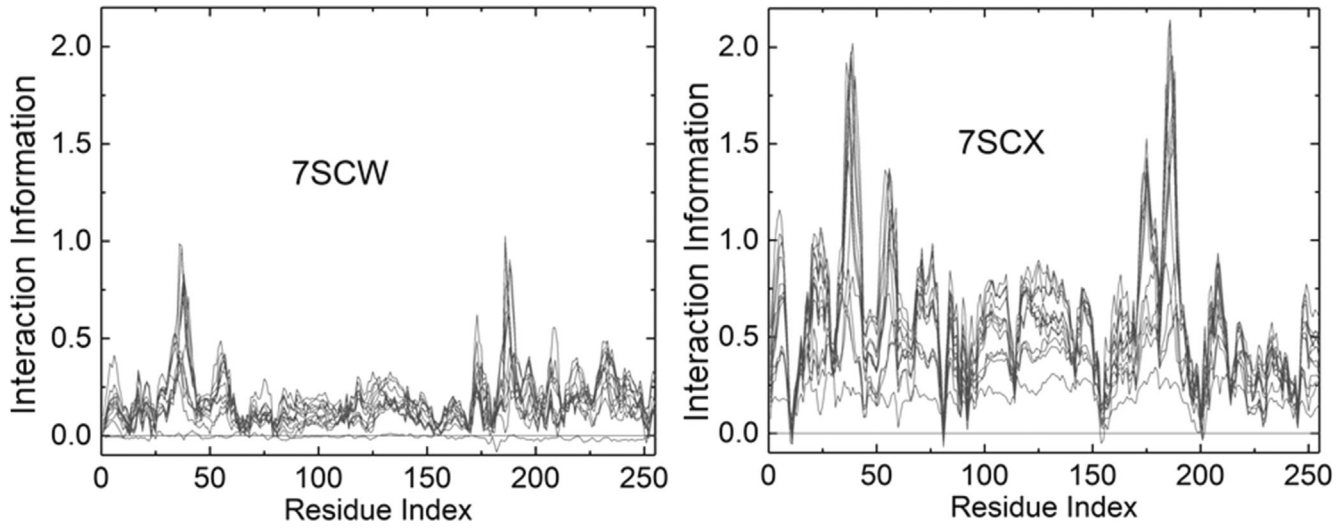

FIGURE 7 Interaction information values superposed for all interface residues. The dominant effect is anti-cooperative, the peaks showing the hotspot regions leading to large anti-cooperativities. Negative values are negligibly small indicating no synergy. Residues 1 to 169 correspond to KRAS, while residues 170 to 255 are attributed to RGL1 (specifically, residues 683 to 768). All curves are obtained using Equation (7).

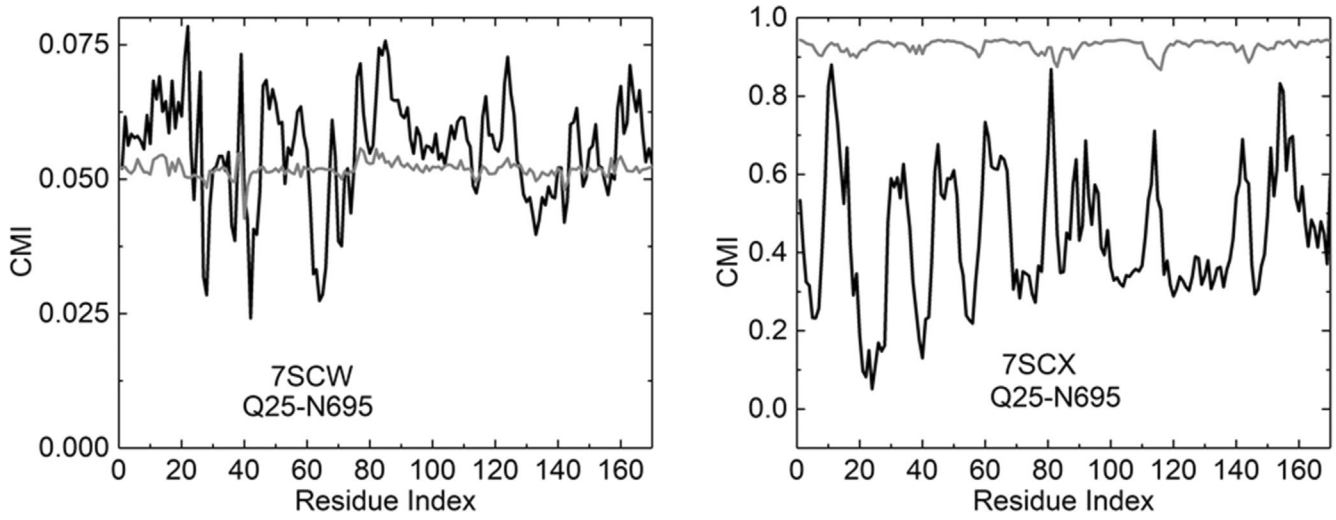

FIGURE 8 Perturbation of the interaction between Q25 and N695 when the fluctuations of residues indexed along the abscissa are suppressed. The fluctuations are suppressed one residue at a time and the resulting CMI is plotted along the ordinate. The left panel is for the wild type complex7SCW, the right panel for 7SCX, the G12V variant. Black and gray curves are values for unsuppressed and suppressed fluctuations, respectively.

4 | CONCLUSIONS AND DISCUSSION

Experimental and clinical evidence shows that each mutation of RAS family proteins participates in distinct signal transduction cascades and has different biological functions.[64,65] For example, the G12V mutation in HRAS, NRAS, KRAS4A, and KRAS4B proteins results in different abilities to activate RAF1, with the G12V mutation in KRAS showing the highest activation. Weng et al[44] showed that allosteric mutations typically inhibit binding to all tested effectors, which contradicts the experimental observation of Voice et al.[64] that G12V increases the activation of RAF1. However, other studies have shown that the G12V mutation does not strengthen the activation of RAF in all cases[66] and is hypothesized to be dependent on cellular context. These and several other observations clearly show that the mutation effects in RAS proteins are specific to the type of mutation and may be context dependent, and therefore each case should be studied individually. The present computational study is based on a single KRAS-RGL1 complex in water.

We see in Figure 1 that MI between interface residues increases upon G12V mutation. This is mainly due to the formation of a more compact structure, that is, a jigsaw-like matching of the components of the complex, upon the G12V mutation. We see in Table 1 that 9 of the 14 interface pairs show a reduction in pair distance upon

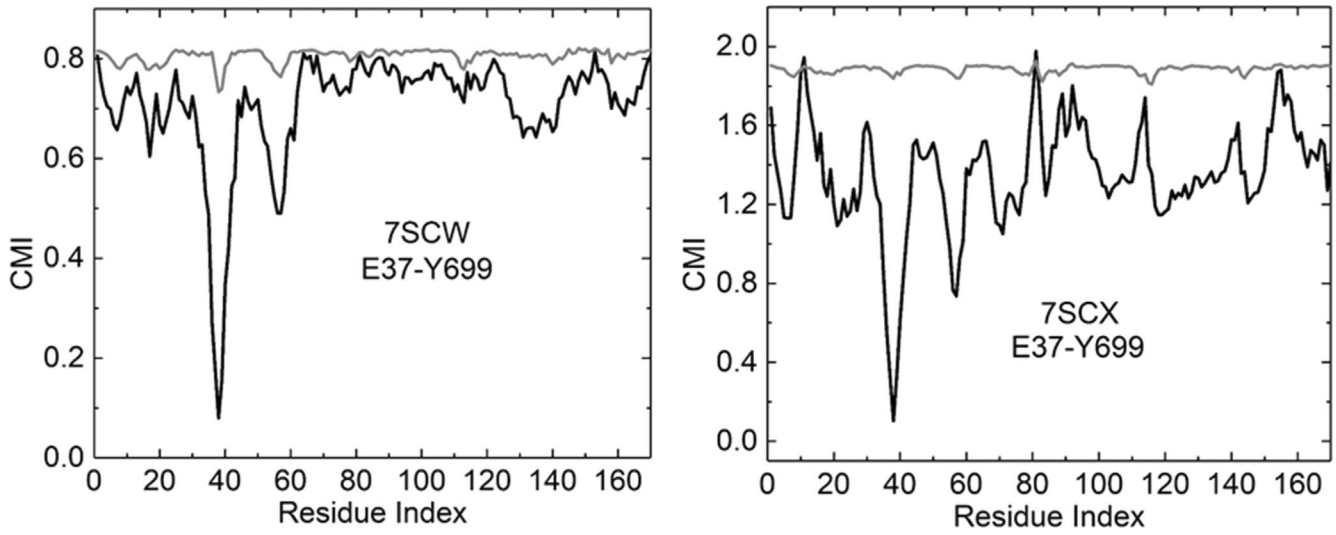

FIGURE 9 Perturbation of the interaction between E37 and Y699 when the fluctuations of residues indexed along the abscissa are suppressed. See legend for Figure 8.

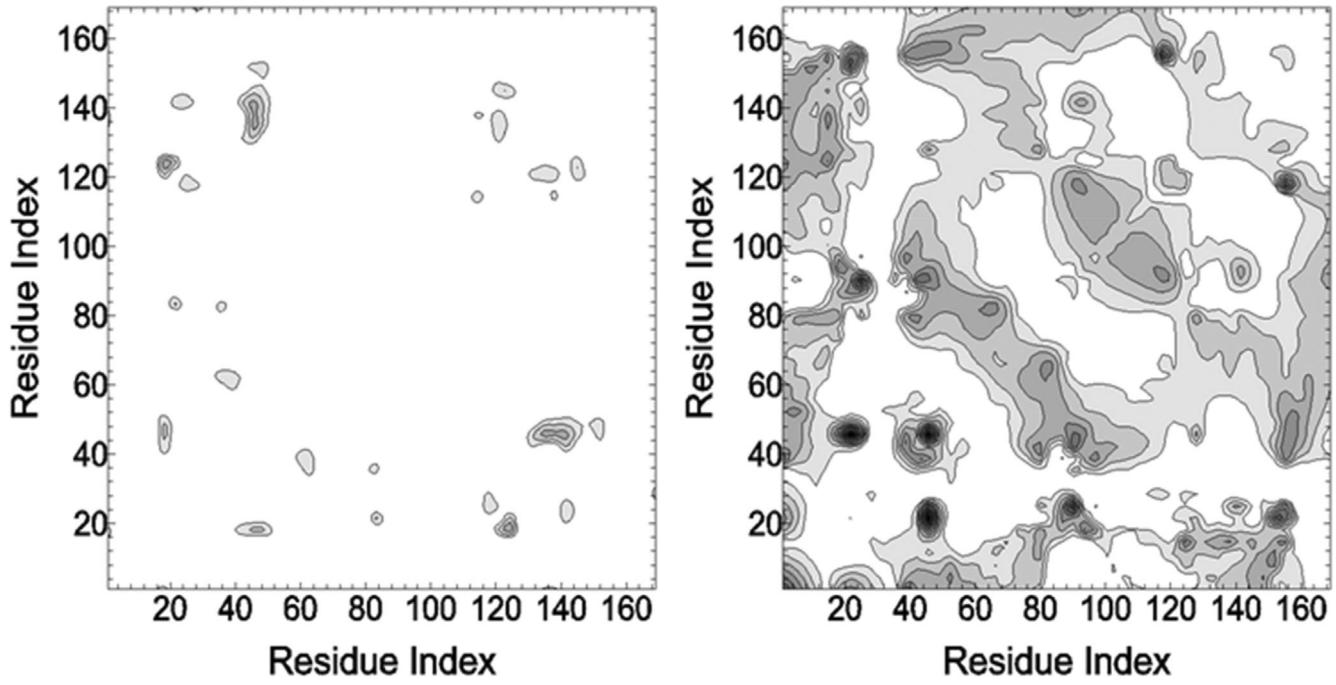

FIGURE 10 Synergistic interaction between all residue pairs (indexed along the abscissa and ordinate) resulting from allosteric effect of residue 12. Only the negative values of interaction information are shown. The left panel is for the WT, right panel for G12V mutant variant. The values are calculated by Equation (7).

mutation. The three pairs where distance increases are shown in gray letters.

Accordingly, we conclude that a larger amount of uncertainty is lost in the $KRAS_{G12V}$-RGL1 complex compared to the wild type complex due to structural change, that is, change in time averaged positions. However, the allosteric activity of a third residue on the complex has opposing effects and increases uncertainty in the mutated complex as may be seen from Figures 3 and 4. Thus, while the G12V mutation increases the stability of the complex, allosteric activity decreases it.

In conclusion, this study explored both MI and II in the context of the KRASG12V-RGL1 complex. MI, quantifying uncertainty lost upon the interaction of two residues, revealed that the G12V mutation increased the MI between interface residues, indicating reduced uncertainty and enhanced correlations due to the formation of a more compact structure in the complex. In parallel, the investigation of II,

TABLE 1 Distance between alpha carbons of interface residue pairs.

Residue i	Pair distance WT (Å)	Pair distance G12V (Å)
Q25-N695	6.841	7.071
E31-N722	10.566	10.682
D33-K700	11.181	11.078
D33-K720	7.508	7.693
P34-K720	9.578	9.711
E37-R688	8.407	8.278
E37-Y699	8.503	8.401
E37-S701	5.391	5.298
D38-Y699	5.794	5.747
D38-S701	5.975	5.974
S39-M698	5.325	5.224
S39-Y699	5.408	5.461
R41-N695	9.107	8.985
R41-G696	5.316	5.205

which considers the influence of a third residue on the interaction of the two interface residues, provided valuable insights into the allosteric effects within the complex. The positive values of II indicated an anti-cooperative influence of the third residue on the interface pair, which can lead to increased uncertainty in the interaction energy. Interestingly, while the G12V mutation increased both MI and II, the net effect on the stability of the complex was still an increase. This suggests that despite the anti-cooperative influence introduced by the third residue, the structural changes brought about by the G12V mutation dominate, leading to a stabilizing effect on the complex.

These findings underscore the complexity of protein–protein interactions, where multiple factors, such as direct residue interactions (MI) and allosteric influences (II), collectively shape the behavior of the complex bringing forth hidden allosteric states and that may lead to the discovery of new mechanisms as addressed by recent studies.[67] The observed increase in stability upon the G12V mutation, despite the anti-cooperative effects, highlights the potential of targeted mutations[68] in modulating protein function. Furthermore, the study's identification of residue D57 as a key contributor to the anti-cooperative interactions of interface residues presents an intriguing avenue for potential therapeutic targeting. The distance between magnesium ion of GDP and the mass center of two oxygen atoms OD1 and OD2 of D57 produces a fluctuation range of 3.40–5.81 Å in the WT KRAS, while this distance fluctuates from 2.22 to 3.38 Å in the G12A and G12R KRAS mutations,[69] indicating that the stability of the magnesium ion in the G12A and G12R KRAS is higher than that in the WT KRAS. Careful exploration of D57's dynamics and functional role is warranted to determine its suitability as a therapeutic target without compromising the overall stability of the complex.

In summary, this research not only advances our understanding of the mutual and interaction information in protein complexes but also provides insights into allosteric regulation and its implications for drug design. The integrated analysis of MI and II has exposed the delicate interplay between residue interactions and allosteric effects, offering novel opportunities to explore and manipulate protein–protein interactions for future therapeutic interventions.[70,71]

AUTHOR CONTRIBUTIONS

Burak Erman: Writing – review and editing; investigation; writing – original draft; formal analysis. **Aysima Hacisuleyman:** Writing – review and editing; investigation; writing – original draft; formal analysis.

PEER REVIEW

The peer review history for this article is available at https://www.webofscience.com/api/gateway/wos/peer-review/10.1002/prot.26657.

DATA AVAILABILITY STATEMENT

The data that support the findings of this study are available from the corresponding author upon reasonable request.

ORCID

Aysima Hacisuleyman https://orcid.org/0000-0003-2471-0296
Burak Erman https://orcid.org/0000-0002-2496-6059

REFERENCES

1. Eves BJ, Gebregiworgis T, Gasmi-Seabrook GM, et al. Structures of RGL1 RAS-Association domain in complex with KRAS and the oncogenic G12V mutant. *J Mol Biol*. 2022;434(9):167527.
2. Smithy JW, O'Reilly EM. Pancreas cancer: therapeutic trials in metastatic disease. *J Surg Oncol*. 2021;123(6):1475-1488.
3. Whaby M, Khan I, O'Bryan JP. Targeting the "undruggable" RAS with biologics. *In Advances in Cancer Research*. 2022;153:237-266.
4. Cunningham BC, Wells JA. High-resolution epitope mapping of hGH-receptor interactions by alanine-scanning mutagenesis. *Science*. 1989;244(4908):1081-1085.
5. LeVine MV, Weinstein H. NbIT-a new information theory-based analysis of allosteric mechanisms reveals residues that underlie function in the leucine transporter LeuT. *PLoS Comput Biol*. 2014;10(5):e1003603.
6. Dunn SD, Wahl LM, Gloor GB. Mutual information without the influence of phylogeny or entropy dramatically improves residue contact prediction. *Bioinformatics*. 2008;24(3):333-340.
7. Weigt M, White RA, Szurmant H, Hoch JA, Hwa T. Identification of direct residue contacts in protein–protein interaction by message passing. *Proc Natl Acad Sci*. 2009;106(1):67-72.
8. LeVine MV, Perez-Aguilar JM, Weinstein H. N-body information theory (NbIT) analysis of rigid-body dynamics in intracellular loop 2 of the 5-HT2A receptor. *arXiv Preprint*. 2014;arXiv:1406.4730.
9. LeVine MV, Weinstein H. AIM for allostery: using the Ising model to understand information processing and transmission in allosteric biomolecular systems. *Entropy*. 2015;17(5):2895-2918.
10. Khelashvili G, Schmidt SG, Shi L, et al. Conformational dynamics on the extracellular side of LeuT controlled by Na+ and K+ ions and the protonation state of Glu290. *J Biol Chem*. 2016;291(38):19786-19799.
11. Khelashvili G, Weinstein H. Functional mechanisms of neurotransmitter transporters regulated by lipid–protein interactions of their terminal loops. *Biochimica et Biophysica Acta (BBA)-Biomembranes*. 2015;1848(9):1765-1774.

12. Quick M, Abramyan AM, Wiriyasermkul P, Weinstein H, Shi L, Javitch JA. The LeuT-fold neurotransmitter: sodium symporter MhsT has two substrate sites. *Proc Natl Acad Sci*. 2018;115(34):E7924-E7931.
13. Stolzenberg S, Quick M, Zhao C, et al. Mechanism of the association between Na+ binding and conformations at the intracellular gate in neurotransmitter: sodium symporters. *J Biol Chem*. 2015;290(22):13992-14003.
14. Stolzenberg S, Michino M, LeVine MV, Weinstein H, Shi L. Computational approaches to detect allosteric pathways in transmembrane molecular machines. *Biochim Biophys Acta*. 2016;1858(7):1652-1662.
15. Khelashvili G, Kots E, Cheng X, Levine MV, Weinstein H. The allosteric mechanism leading to an open-groove lipid conductive state of the TMEM16F scramblase. *Commun Biol*. 2022;5(1):990.
16. LeVine MV, Cuendet MA, Khelashvili G, Weinstein H. Allosteric mechanisms of molecular machines at the membrane: transport by sodium-coupled symporters. *Chem Rev*. 2016;116(11):6552-6587.
17. Khelashvili G, Stanley N, Sahai MA, et al. Spontaneous inward opening of the dopamine transporter is triggered by PIP2-regulated dynamics of the N-terminus. *ACS Chem Nerosci*. 2015;6(11):1825-1837.
18. Osei-Owusu J, Kots E, Ruan Z, et al. Molecular determinants of pH sensing in the proton-activated chloride channel. *Proc Natl Acad Sci*. 2022;119(31):e2200727119.
19. Abramyan AM, Stolzenberg S, Li Z, Loland CJ, Noé F, Shi L. The isomeric preference of an atypical dopamine transporter inhibitor contributes to its selection of the transporter conformation. *ACS Chem Nerosci*. 2017;8(8):1735-1746.
20. Meral D, Provasi D, Filizola M. An efficient strategy to estimate thermodynamics and kinetics of G protein-coupled receptor activation using metadynamics and maximum caliber. *J Chem Phys*. 2018;149(22):224101.
21. Marino KA, Shang Y, Filizola M. Insights into the function of opioid receptors from molecular dynamics simulations of available crystal structures. *Br J Pharmacol*. 2018;175(14):2834-2845.
22. Schneider S, Provasi D, Filizola M. How oliceridine (TRV-130) binds and stabilizes a μ-opioid receptor conformational state that selectively triggers G protein signaling pathways. *Biochemistry*. 2016;55(46):6456-6466.
23. Bozzi AT, McCabe AL, Barnett BC, Gaudet R. Transmembrane helix 6b links proton and metal release pathways and drives conformational change in an Nramp-family transition metal transporter. *J Biol Chem*. 2020;295(5):1212-1224.
24. Barth P, Senes A. Toward high-resolution computational design of the structure and function of helical membrane proteins. *Nat Struct Mol Biol*. 2016;23(6):475-480.
25. Plante, E. *Examination of the Effects of Myosin-1e Expression on Tumor Behavior and Computational Analysis of MYO1E Mutations Associated with Kidney Disease (Doctoral dissertation)*. 2022.
26. Karami Y, Bitard-Feildel T, Laine E, Carbone A. "Infostery" analysis of short molecular dynamics simulations identifies highly sensitive residues and predicts deleterious mutations. *Sci Rep*. 2018;8(1):1-18.
27. Habgood M, Seiferth D, Zaki A-M, Alibay I, Biggin PC. Atomistic mechanisms of human TRPA1 activation by electrophile irritants through molecular dynamics simulation and mutual information analysis. *Sci Rep*. 2022;12(1):4929.
28. Focht D, Neumann C, Lyons J, et al. A non-helical region in transmembrane helix 6 of hydrophobic amino acid transporter MhsT mediates substrate recognition. *EMBO J*. 2021;40(1):e105164.
29. Moal IH, Fernández-Recio J. SKEMPI: a structural kinetic and energetic database of mutant protein interactions and its use in empirical models. *Bioinformatics*. 2012;28(20):2600-2607.
30. Thorn KS, Bogan AA. ASEdb: a database of alanine mutations and their effects on the free energy of binding in protein interactions. *Bioinformatics*. 2001;17(3):284-285.
31. Kumar MS, Gromiha MM. PINT: protein–protein interactions thermodynamic database. *Nucleic Acids Res*. 2006;34(suppl_1):D195-D198.
32. Pantsar T. The current understanding of KRAS protein structure and dynamics. *Comput Struct Biotechnol J*. 2020;18:189-198.
33. Ostrem JM, Shokat KM. Direct small-molecule inhibitors of KRAS: from structural insights to mechanism-based design. *Nat Rev Drug Discov*. 2016;15(11):771-785.
34. McCormick F. KRAS as a therapeutic target. *Clin Cancer Res*. 2015;21(8):1797-1801.
35. Parikh K, Banna G, Liu SV, et al. Drugging KRAS: current perspectives and state-of-art review. *J Hematol Oncol*. 2022;15(1):152.
36. Wang H, Chi L, Yu F, et al. Annual review of KRAS inhibitors in 2022. *Eur J Med Chem*. 2023;249:115124.
37. Seton-Rogers S. KRAS-G12C in the crosshairs. *Nat Rev Cancer*. 2020;20(1):3.
38. Huang L, Guo Z, Wang F, Fu L. KRAS mutation: from undruggable to druggable in cancer. *Signal Transduct Target Ther*. 2021;6(1):386.
39. Jančík S, Drábek J, Radzioch D, Hajdúch M. Clinical relevance of KRAS in human cancers. *J Biomed Biotechnol*. 2010;2010:1-13.
40. Gorfe AA, Cho K-J. Approaches to inhibiting oncogenic K-Ras. *Small GTPases*. 2021;12(2):96-105.
41. Campitelli P, Modi T, Kumar S, Ozkan SB. The role of conformational dynamics and allostery in modulating protein evolution. *Annu Rev Biophys*. 2020;49:267-288.
42. Ostrem JM, Peters U, Sos ML, Wells JA, Shokat KM. K-Ras (G12C) inhibitors allosterically control GTP affinity and effector interactions. *Nature*. 2013;503(7477):548-551.
43. Lito P, Solomon M, Li L-S, Hansen R, Rosen N. Allele-specific inhibitors inactivate mutant KRAS G12C by a trapping mechanism. *Science*. 2016;351(6273):604-608.
44. Weng C, Faure AJ, Lehner B. The energetic and allosteric landscape for KRAS inhibition. *bioRxiv*. 2022;2022.12.06.519122. https://doi.org/10.1101/2022.12.06.519122
45. Jo S, Kim T, Iyer VG, Im W. CHARMM-GUI: a web-based graphical user interface for CHARMM. *J Comput Chem*. 2008;29(11):1859-1865.
46. Jorgensen WL, Chandrasekhar J, Madura JD, Impey RW, Klein ML. Comparison of simple potential functions for simulating liquid water. *J Chem Phys*. 1983;79(2):926-935.
47. Feller SE, Zhang Y, Pastor RW, Brooks BR. Constant pressure molecular dynamics simulation: the Langevin piston method. *J Chem Phys*. 1995;103(11):4613-4621.
48. Phillips JC, Hardy DJ, Maia JD, et al. Scalable molecular dynamics on CPU and GPU architectures with NAMD. *J Chem Phys*. 2020;153(4):044130.
49. Callen HB. *Thermodynamics and an Introduction to Thermostatistics*. 2nd ed. Wiley; 1985.
50. Demirtas K, Erman B, Haliloglu T. Dynamic allostery in proteins: exact and approximate methods for evaluating mutual information from molecular dynamics trajectories. *J Chem Theory Comput*. 2023.
51. McClendon CL, Friedland G, Mobley DL, Amirkhani H, Jacobson MP. Quantifying correlations between allosteric sites in thermodynamic ensembles. *J Chem Theory Comput*. 2009;5(9):2486-2502.
52. Kumar A, Glembo TJ, Ozkan SB. The role of conformational dynamics and allostery in the disease development of human ferritin. *Biophys J*. 2015;109(6):1273-1281.
53. Ose NJ, Butler BM, Kumar A, et al. Dynamic coupling of residues within proteins as a mechanistic foundation of many enigmatic pathogenic missense variants. *PLoS Comput Biol*. 2022;18(4):e1010006.
54. Atilgan C, Atilgan AR. Perturbation-response scanning reveals ligand entry-exit mechanisms of ferric binding protein. *PLoS Comput Biol*. 2009;5(10):e1000544.
55. Erman B. A computational model for controlling conformational cooperativity and function in proteins. *Proteins*. 2018;86(9):1001-1009.

56. Erkip A, Erman B. Dynamics of large-scale fluctuations in native proteins. Analysis based on harmonic inter-residue potentials and random external noise. *Polymer*. 2004;45(2):641-648.
57. Haliloglu T, Seyrek E, Erman B. Prediction of binding sites in receptor-ligand complexes with the Gaussian network model. *Phys Rev Lett*. 2008;100:228102-228104.
58. Bahar I, Atilgan AR, Demirel MC, Erman B. Vibrational dynamics of folded proteins: significance of slow and fast motions in relation to function and stability. *Phys Rev Lett*. 1998;80(12):2733-2736.
59. Lange OF, Grubmüller H. Generalized correlation for biomolecular dynamics. *Proteins*. 2006;62(4):1053-1061.
60. Erman B. Mutual information analysis of mutation, nonlinearity, and triple interactions in proteins. *Proteins*. 2023;91(1):121-133.
61. Stephen AG, Esposito D, Bagni RK, McCormick F. Dragging ras back in the ring. *Cancer Cell*. 2014;25(3):272-281.
62. Prior IA, Lewis PD, Mattos C. A comprehensive survey of Ras mutations in cancer. *Cancer Res*. 2012;72(10):2457-2467.
63. Pylayeva-Gupta Y, Grabocka E, Bar-Sagi D. RAS oncogenes: weaving a tumorigenic web. *Nat Rev Cancer*. 2011;11(11):761-774.
64. Voice JK, Klemke RL, Le A, Jackson JH. Four human ras homologs differ in their abilities to activate Raf-1, induce transformation, and stimulate cell motility. *J Biol Chem*. 1999;274(24):17164-17170.
65. Muñoz-Maldonado C, Zimmer Y, Medová M. A comparative analysis of individual RAS mutations in cancer biology. *Front Oncol*. 2019;9:1088.
66. Hunter JC, Manandhar A, Carrasco MA, Gurbani D, Gondi S, Westover KD. Biochemical and structural analysis of common cancer-associated KRAS mutations. *Mol Cancer Res*. 2015;13(9):1325-1335.
67. Verkhivker GM. Making the invisible visible: toward structural characterization of allosteric states, interaction networks, and allosteric regulatory mechanisms in protein kinases. *Curr Opin Struct Biol*. 2021;71:71-78.
68. Vatansever S, Erman B, & Gümüş Z.H Oncogenic G12D mutation alters local conformations and dynamics of K-Ras. *Sci Rep*. 2019;9:11730.
69. Shi S, Zheng L, Ren Y, Wang Z. Impacts of mutations in the P-loop on conformational alterations of KRAS investigated with Gaussian accelerated molecular dynamics simulations. *Molecules*. 2023;28(7):2886.
70. Pálfy G, Menyhárd DK, Perczel A. Dynamically encoded reactivity of Ras enzymes: opening new frontiers for drug discovery. *Cancer Metastasis Rev*. 2020;39(4):1075-1089.
71. Ratnasinghe BD, Haque N, Wagenknecht JB, et al. Beyond structural bioinformatics for genomics with dynamics characterization of an expanded KRAS mutational landscape. *bioRxiv*. 2023. https://doi.org/10.1101/2023.04.28.536249

SUPPORTING INFORMATION

Additional supporting information can be found online in the Supporting Information section at the end of this article.

How to cite this article: Hacisuleyman A, Erman B. Synergy and anti-cooperativity in allostery: Molecular dynamics study of WT and oncogenic KRAS-RGL1. *Proteins*. 2024;92(5):665-678. doi:10.1002/prot.26657